INFLUENCE OF BLADE SWEEP ON AERODYNAMICS AND ACOUSTICS OF LOW-PRESSURE AXIAL FANS

Alexander SKORPEL, Philip FRANTZHELD,
Jens FRIEDRICHS

TU Braunschweig, Institute of Jet Propulsion and Turbomachinery,
Hermann-Blenk-Straße 37, 38108 Braunschweig, Germany

SUMMARY

Literature shows a strong effect of blade sweep on the acoustics of axial fans. Starting with a swept fan as a reference two new fans were build following the same design process but with different sweep parameters (max sweep at tip/radial shape of sweep). Fan characteristics and the corresponding sound emissions were measured. Further, wall pressure measurements show characteristics of the tip vortex as a strong source of sound in this application. The aerodynamic measurements are compared to RANS-simulations and show a proper accordance.

NOMENCLATURE

Latin symbols

A, B	form parameters
c	absolute velocity
D	diameter
s	shift distance
p	pressure
P	power
r	radius
R	dimensionless radius r/r_{tip}
u	circumferential velocity
$\dot{V}$	volume flow rate
x	axial coordinate

Greek symbols

δ	shift angle
η	efficiency
φ	flow coefficient
ϕ	sweep angle
Ψ	pressure rise coefficient
ρ	density
Θ	azimuthal angle
ν	hub-to-tip ratio

INTRODUCTION

Low pressure axial fans are used in various industrial and private applications such as ventilation systems and heat exchangers in facilities and the automotive sector. A vast amount of energy is consumed by the still increasing demand for all kinds of fans. At the same time the requirement for better aeroacoustics is also increasing. So the main objectives of modern design approaches are high efficiency at low sound emissions. The design approach used in this case study was presented by Lindemann [1], [2]. It allows to apply sweep to a so far unswept blade while compensating for the reduction of section lift [3] by increasing the chord length. He showed that a moderate blade sweep could lead to a significant noise reduction of up to 8.0 dB(A). As the blade tip vortex is a dominant source of sound in this configuration [4] a special focus is set on the blade tip region. The tip vortex is strongly influenced by the pressure difference between pressure and suction side and the gap height. The gap height is set to a constant value of $t_{\text{gap}} = 3\,\text{mm}$. The local pressure difference between pressure and suction side can be influenced by sweep. Therefore variations in the radial shape of sweep will have an effect on the blade tip vortex. By measuring the static casing wall pressure this effect can be observed. To assess the different designs acoustic measurements are carried out in an anechoic chamber by an industrial partner.

METHODOLOGY

Fan design

All fans presented in this paper have an outer diameter of $D = 497\,\text{mm}$ and a hub-to-shroud ratio of 0.3. They are designed for pureley axial inlet velocities. The blades have a constant thickness of 4 mm. Leading and trailing edge are rounded with constant radius of 2 mm. All fans have 5 blades with the same chord length distribution at the beginning of the design process. The chord length changes whenever sweep is applied to compensate for reduced section lift.

Sweep in the present study is realized by applying a chordwise shift to the blade sections. A positive shift results in a backward sweep and vice versa. The shift of the center of gravity is controlled by the shift angle δ:

$$\frac{\delta}{\delta_{\text{max}}} = e^{AR^B} - e^{A\nu^B}$$

with the hub-to-tip ratio $\nu = D_h/D$. A and B are free form parameters to adjust the desired sweep. R is the dimensionless radius r/r_{tip}. The local sweep angle can then be calculated by:

$$\tan\phi(r) = \frac{\Delta s(r)/r_T}{\Delta R}\,,$$

where Δs is the shift difference between two adjacent blade sections (see Fig 1).

Using the parameters from Table 1 three different shapes for ϕ were used to design a new fan. Fan V1 is the baseline configuration. The design parameters are exactly the same ones that were used in former investigations achieving good acoustic results. The only difference is the increase of blade thickness from 2 mm to 4 mm so the blades are capable of mounting pressure transducers in the future.

The intention while creating fan V2 was to evaluate the influence of maximum sweep at blade tip on the tip clearance vortex and the acoustics. It was obeserved, that the larger the maximum sweep angle the lower the acoustic emissions. Therfore fan V2 aimed for a higher maximum sweep angle compared to V1 (see Fig. 2). Fan V3 is very similar to the reference fan V1. There is no sweep up to $R = 0.6$ but then catches up to the same value as V1 at the blade tip. This results in a bulkier shape in

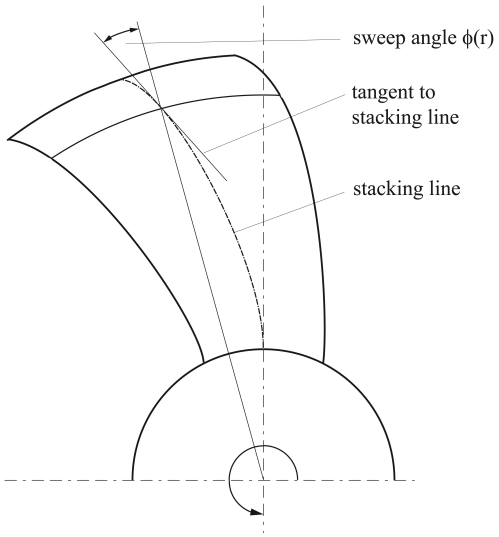

Figure 1: Definition of sweep angle ϕ; Axial Projection [1]

Table 1: Fan design parameters

	A	B	ν	$\delta_{\max}/[°]$	$\phi_{\max}/[°]$	$r_{\text{tip}}/[mm]$	n_{Blades}
Fan V1	0.72	2	0.3	30	57	248.5	5
Fan V2	0.72	2	0.65	72	75	248.5	5
Fan V3	1.04	1	0.6	30	57	248.5	5

the upper third of the blade. As the reduced section lift is compensated by an increase in chord length fan V2 is much longer at the tip, V1 and V2 only show slight differences between $0.5 < R < 0.85$ ending in the exact same tip geometry, see Fig (3).

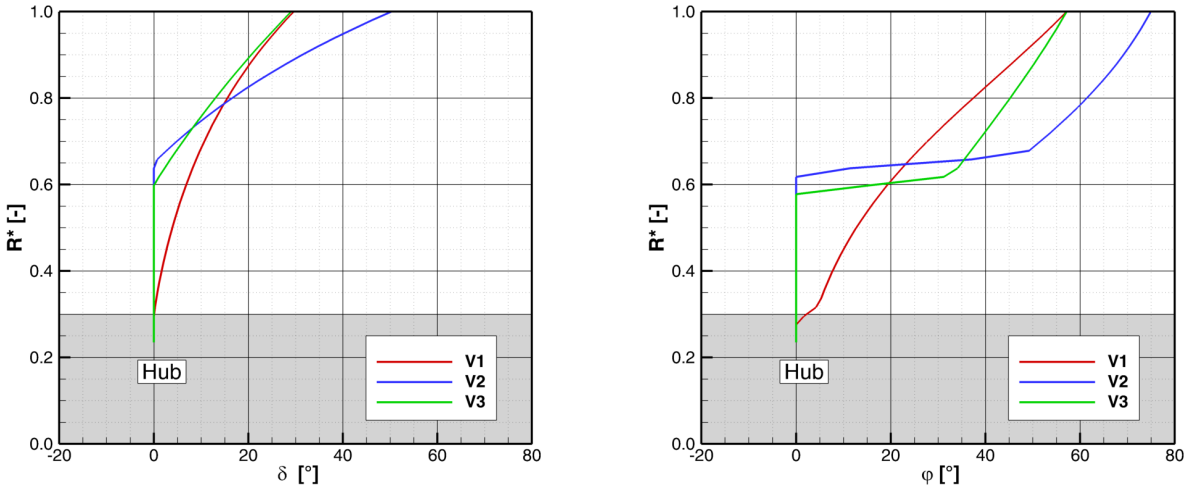

(a) Shift angle δ (b) Sweep angle ϕ

Figure 2: Radial distribution of shift angle (a) and the resulting sweep angle (b) for fans V1-V3

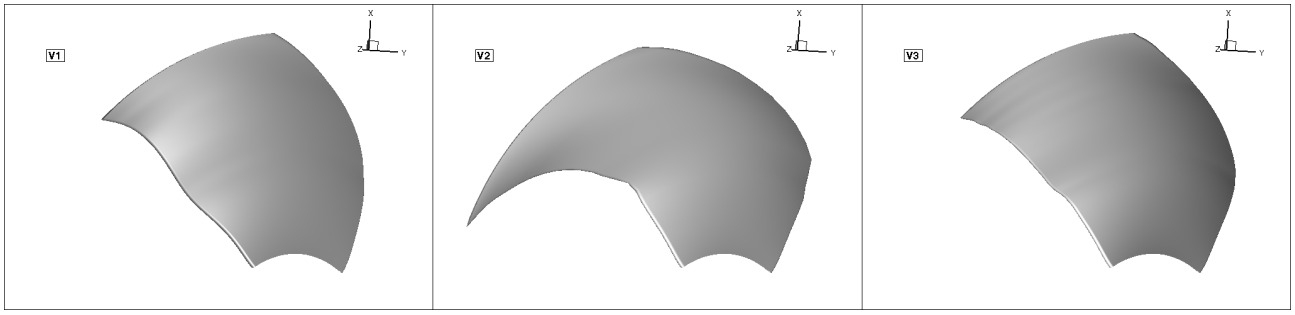

Figure 3: Geometry of fan blades V1-V3

Experimental Setup

All fans are tested in a free inlet and outlet test chamber setup according to DIN/ISO5801. A full-length nozzle with a diameter $D_{\text{nozzle}} = 503\,\text{mm}$ was installed. The orifice is extended by a tube of constant diameter to provide wall pressure and PIV measurements close to the blade tip. Motor, torque measurement drive shaft and tachometer are positioned upstream. This setup allows the measurement of fan characteristics in terms of flow coefficient φ, total-to-static pressure rise coefficient Ψ_{ts} and total-to-static efficiency η_{ts}, see Eqn. (1-3).

$$\varphi = \frac{\dot{V}}{\pi \frac{1}{4}(D_{\text{tip}}^2 - D_{\text{hub}}^2) \cdot u_{\text{tip}}} \tag{1}$$

$$\Psi_{\text{ts}} = \frac{\Delta p_{\text{ts}}}{\frac{\rho}{2} u_{\text{tip}}^2} \tag{2}$$

$$\eta_{\text{ts}} = \frac{\dot{V} \cdot \Delta p_{\text{ts}}}{P_{\text{mech}}} \tag{3}$$

In addition, the exit stream velocities were measured in a constant axial position of 7 mm behind the fan hub which approximately aligns with blade trailing edge at its maximum extent using a 5-hole-probe measurement setup. The radial resolution is $\Delta r = 5\,\text{mm}$.

To characterize the blade tip vortex a traversible wall flush-mounted pressure transducer is used. 1024 values per revolution were measured resulting in circumferential resolution of approximately 1.5 mm. The axial position of the transducer was changed in same intervalls of $\Delta x = 1.5\,\text{mm}$ resulting in an almost equidistant measurement matrix. The ensamble-averaged ($n_{\text{rev}} = 64$) static pressure and the corresponding standard deviation were calculated according to equations Eqn. (4-5).

$$\bar{p}(x, \Theta) = \frac{1}{n_{\text{rev}}} \sum_{i=1}^{n_{\text{rev}}} p_i(x, \Theta) \tag{4}$$

$$\bar{p}_{\text{RMS}}(x, \Theta) = \sqrt{\frac{1}{n_{\text{rev}}} \sum_{i=1}^{n_{\text{rev}}} \left[p_i\left(x, \Theta\right) - \bar{p}\left(x, \Theta\right) \right]^2} \tag{5}$$

The static pressure measurements are shown using the dimensionless pressure coefficient:

$$\bar{c}_p = \frac{\bar{p}}{\frac{\rho}{2} u_{\text{tip}}^2} \tag{6}$$

$$\bar{c}_{p,RMS} = \frac{\bar{p}_{\text{RMS}}}{\frac{\rho}{2} u_{\text{tip}}^2} \tag{7}$$

Numerical Setup

In addition to the experiments numerical investigations were carried out. The simulated geometry consists of three domains: (1) test chamber with nozzle (90°), (2) fan inside measurement tube and (3) free exhaust part. The axial length of the test chamber was set to twice the fan diameter (2xD), the cross section uses the real dimensions of 1.8 m x 1.8 m. The exhaust domain was set to an axial length of 4xD and radial extension of 3xD to allow for the jet to mix with the environment. The meshing for these domains was done using ANSYS ICEM CFD. For meshing the different fan versions NUMECA Autogrid was used. All grids are of structered type achieving a good overall quality. The average overall grid size was about 5.5 million elements leading to a verified grid independence. ANSYS CFX is used as a solver for reynolds-averaged-navier-stokes (RANS) equations using the SST turbulence model. Regarding the boundary conditions, total pressure at inlet and static pressure at outlet were applied.

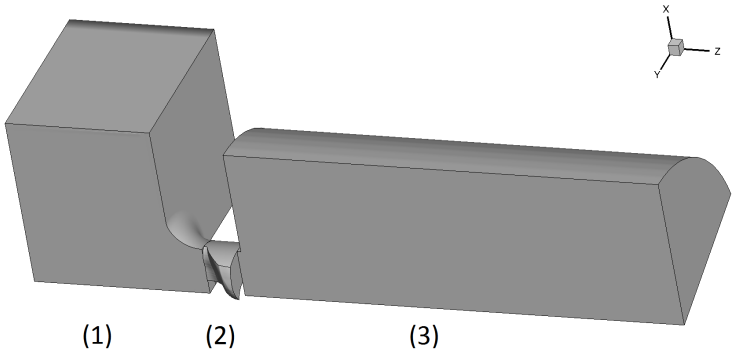

Figure 4: Numerical Setup: (1) test chamber (1:1 scale) with total pressure boundary condition at inlet, (2) fan (72° segment) , (3) outlet region with static pressure boundary condition

RESULTS

Fan characteristics - Experiment / Numerics

Fig. (5a) shows the measured fan characteristics for V1-V3. V1 reaches a very good peak efficiency of 54% at $\varphi = 0.21$ as expected from former experiments. The changes in the radial distribution of sweep angle between V1 and V3 causes a slightly reduced volume flow below $\Psi_{\text{ts}} = 0.25$. Peak efficiency remains unchanged. V2 shows disappointing aerodynamic performance. The volume flow is decreased at all pressure levels. The peak efficiency drops by 2 percentage points and is moved to a smaller volume flow rate. By looking at the exit stream velocities in Fig. (5c) it can be seen that the axial velocity component c_x is much smaller in the outer blade regions. The circumferential velocity c_u and therefore the pressure rise is also lower compared to V1 and V3. In the midsection the radial velocity is negative. This is an indicator for blockage in the upper blade region caused by seperation. This also explains the lower axial component. The intention for designing V2 was to find the limit of this design process and it seems that the extreme sweep exceeded this limit. The CFD simulations of V1 and V3 show a very good agreement with the experimental data, see Fig. (5b). It can be seen that above $\Psi = 0.2$ no converging soulution could be achieved for V2. This supports the assumption of a growing seperation hence a strong unsteady phenomenon that cannot be solved using RANS. Nevertheless the good agreement for V1 and V3 is a good verification for the setup. This opens the opportunity to use CFD as a cost effective method for fan design opitmization.

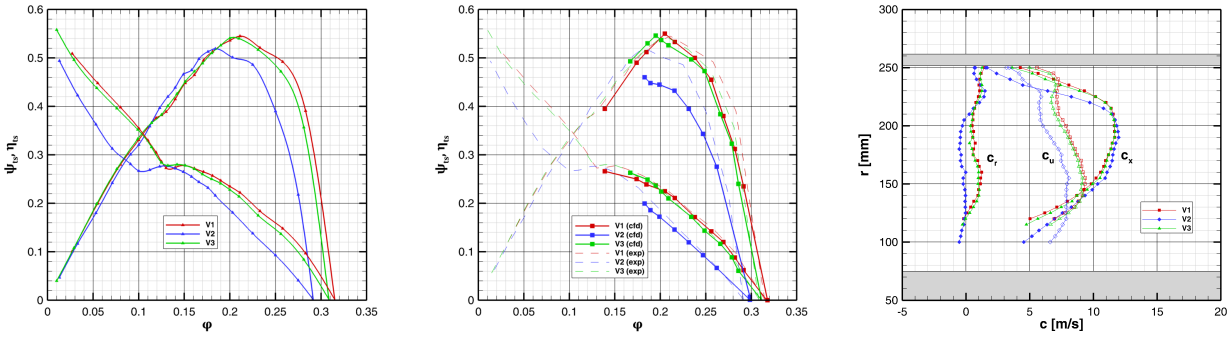

(a) Fan characteristics (EXP) (b) Fan characteristics (CFD) (c) 5-hole-probe measurements

Figure 5: Fan characteristics and exit stream velocities at design point

Wall Pressure Comparison

Fig. (6a) shows the non-dimensional static wall pressure in the fan casing at four different operating points for V1. The white line represents the approximate position of the blade tip. Close to this line there is a local pressure maximum and minimum representing the surface pressure on both sides of the blade tip. Looking at $\varphi = 0.27$ there is a distinct red line of low pressure swerving from the blade suction side. This shows the blade tip clearance vortex. The clearance vortex of the adjacent blade coming from the bottom passes the trailing edge. With decreasing φ the angle changes and the vortex barely hits the trailing edge. At $\varphi = 0.19$ and $\varphi = 0.15$ this disctinct structure becomes more blurred and until the vortex breaks down. This comes along with an increase of the measured pressure standard deviation, see Fig. (6b).

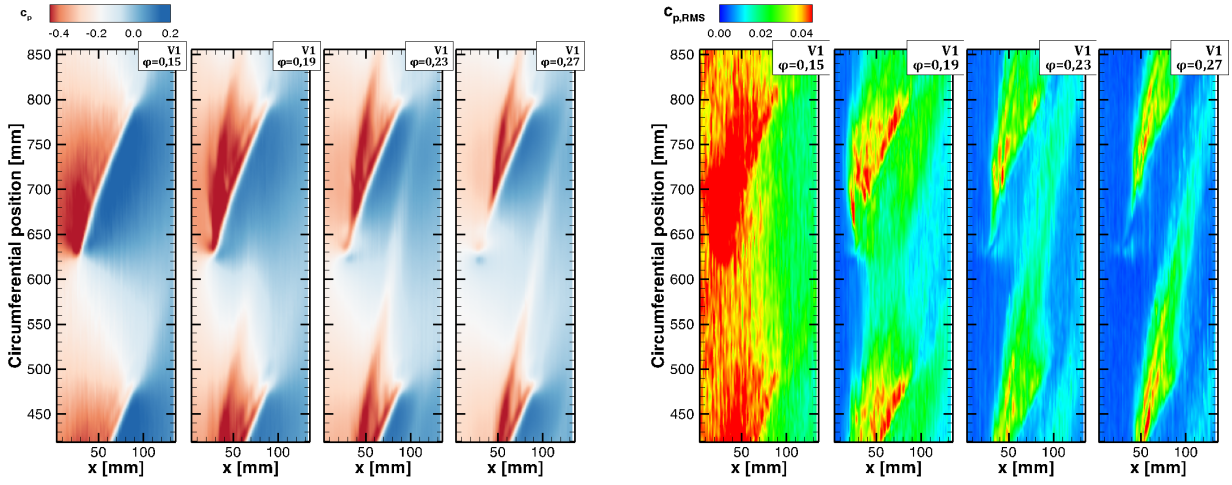

(a) Non-dimensional wall pressure (b) Standard deviation of wall pressure

Figure 6: Influence of operating point on wall pressure distribution for fan V1

Fig. (7) shows the wall pressure for all fans at design point. As V1 and V3 have the same sweep angle at the tip and therefore the geometry is identical the pressure map should be nearly identical. The qualitative behaviour, especially the position of tip clearance vortex is the same. V2 has a larger sweep angle at the blade tip. The reduced lift -compensated by a longer chord length (see bottom part)- is visible by smaller absolute pressure values.

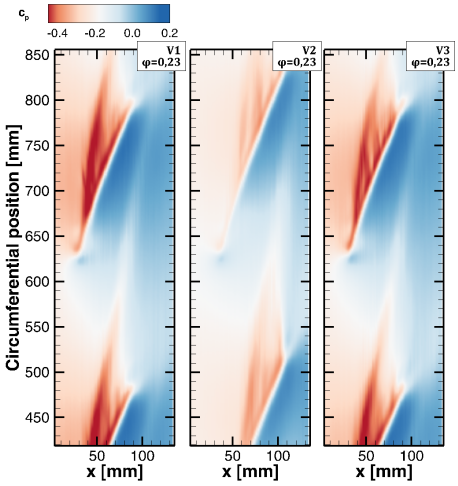

Figure 7: Comparison of fans V1-V3: Wall pressure at design point

Acoustic Comparison

Figure (8a) shows the sound power levels as measured without weighting. V1 and V3 show a very similar behaviour with only small differences of up to 1.5 dB. The strong increase of sound emissions below $\varphi = 0.2$ is traced back to the aforementioned start of tip clearance vortex breakdown. V2 seems to be less noisy at part load but that ignores the much smaller volume flow rate. To compensate for different volume flow rates and pressure rises a specific sound power level is shown in Fig (8b) using the formula:

$$L_{\text{spec.}} = L_{\text{W}} - 10 \log \frac{\dot{V}}{\dot{V}_0} - 20 \log \frac{\Delta p_{\text{fa}}}{\Delta p_{\text{fa,0}}}$$

with $\dot{V}_0 = 1\,\text{m}^3/\text{s}$ and $\Delta p_{\text{fa,0}} = 1\,\text{Pa}$ (see Carolus [5]) . It can be seen that V1 shows the best results at design point. V3 is still about 1 dB louder. V2 hat its minimum at $\varphi = 0.19$.

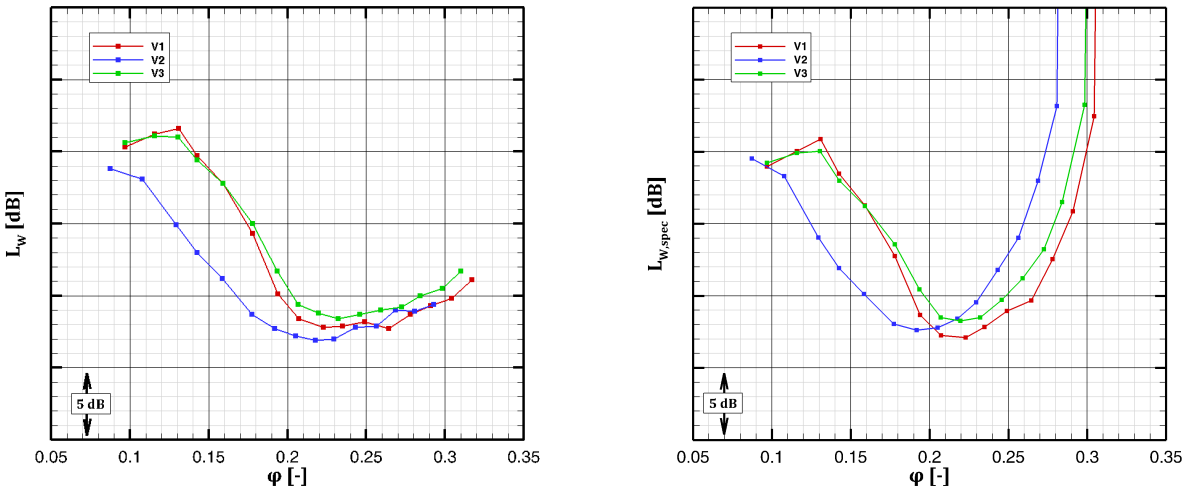

(a) Sound Power Level

(b) Specific Sound Power Level

Figure 8: Comparison of sound emissions of fans V1-V3

DISCUSSION AND OUTLOOK

A design method was tested by designing three fans with different sweep. The effect that sweep at the blade tip influences the generation of the tip clearance vortex could be shown. V1 and V3 -two very similar fan designs- do not show differences in the tip clearance vortex structure analyzed by wall pressure measurements. Nevertheless there is a measurable difference in the acoustic emissions. Although wall pressure measurements are a good method to characterize the mean location of the tip clearance vortex they fail at indicating the radial extent of the vortex area. To get more information about the complex secondary flow effects stereo PIV measurements are scheduled. In addition V1 will be equipped with high response pressure tansducers close to the leading edge to gain information about the unsteady inflow pressure field. Sensors in the rear part of the pressure side will detect the impingement of the vortex of the adjacent blade. The numerical setup showed a good agreement with the experimental data and could therfore be validated. As all experimental data showed in this study was averaged no unsteady effects could be shown, yet. This will be done by unsteady CFD focussing on secondary flow effects at the tip clearance.

REFERENCES

[1] Thore Lindemann, Jens Friedrichs, and Udo Stark. *Development Of A New Design Method For High Efficiency Swept Low Pressure Axial Fans With Small Hub Ratio*. In *Proceedings of ASME Turbo Expo 2014*, **2014**.

[2] Thore Lindemann, Jens Friedrichs, and Udo Stark. *Development Of A New Design Approach For High Effficiency Low Pressure Axial Fans With Small Hub Ratio*. In *15th International Conference on Fluid Flow Technologies*, **2012**.

[3] Hermann Schlichting and Erich A. Truckenbrodt. *Aerodynamik des Flugzeuges*. Springer-Verlag Berlin Heidelberg, **1969**.

[4] Frank Kameier and Wolfgang Neise. *Experimental Study of Tip Clearance Losses and Noise in Axial Turbomachines and Their Reduction*. J. Turbomach 119(3), **1997**.

[5] Thomas Carolus. *Ventilatoren - Aerodynamischer Entwurf, Schallvorhersage, Konstruktion.* Springer Vieweg, **2013**.

ACKNOWLEDGEMENTS

The authors would like to thank the research association Forschungsvereinigung für Luft- und Trocknungstechnik (FLT) e.V. for financial support of the research project AiF-Nr.: 18836 N/1. This project is carried out under the auspices of Federation of Industrial Research Associations (AIF) and financed within the budget of the Federal Ministry of Economics and Technology Germany (BMWi).